



Recovery of metals from spent lithium-ion batteries with organic acids as leaching reagents and environmental assessment

Li Li ^{a,c}, Jennifer B. Dunn ^b, Xiao Xiao Zhang ^a, Linda Gaines ^b, Ren Jie Chen ^a, Feng Wu ^{a,*}, Khalil Amine ^{c,**}

^a School of Chemical Engineering and the Environment, Beijing Institute of Technology, Beijing 100081, China

^b Energy Systems Division, Argonne National Laboratory, Argonne, IL 60439, USA

^c Chemical Sciences and Engineering Division, Argonne National Laboratory, IL 60439, USA

HIGHLIGHTS

- A leaching process for the recovery of cobalt and lithium from LIBs was developed.
- Citric and malic acids are more effective as leaching reagents than aspartic acid.
- An environmental assessment was conducted to examine its energy consumption.
- An environmental analysis predicts a FFC energy intensity of recovered Co.
- The technical process is promising and economic with environmental merits.

ARTICLE INFO

Article history:

Received 17 October 2012

Accepted 13 December 2012

Available online 1 February 2013

Keywords:

Spent lithium-ion batteries

Acid leaching

Cathode active materials

Organic acids

Environmental assessment

ABSTRACT

A leaching process for the recovery of cobalt and lithium from spent lithium-ion batteries (LIB) is developed in this work. Three different organic acids, namely citric acid, malic acid and aspartic acid, are used as leaching reagents in the presence of hydrogen peroxide. The cathode active materials before and after acid leaching are characterized by X-ray diffraction and scanning electron microscopy. Recovery of cobalt and lithium is optimized by varying the leachant and H_2O_2 concentrations, the solid-to-liquid ratio, and the reaction temperature and duration. Whereas leaching with citric and malic acids recovered in excess of 90% of cobalt and lithium, leaching with aspartic acid recovered significantly less of these metals. The leaching mechanism likely begins with the dissolution of the active material ($LiCoO_2$) in the presence of H_2O_2 followed by chelation of Co(II) and Li with citrate, malate or aspartate. An environmental analysis of the process indicates that it may be less energy and greenhouse gas intensive to recover Co from spent LIBs than to produce virgin cobalt oxide.

© 2013 Elsevier B.V. All rights reserved.

1. Introduction

Applications of lithium-ion batteries (LIBs) as electrochemical power sources in consumer electronics and electric vehicles (EV) are increasing. LIBs have been available on the market from Sony Corp. since the early 1990s. [1] Desirable characteristics such as modest size and weight, high cell voltage, low self-discharge rates and significantly higher energy density have made LIBs preferable to typical nickel–cadmium or nickel–metal hydride batteries for mobile phones, laptops, electronic devices, and EVs. Graphite– $LiCoO_2$ has become the leading LIB system, which at present powers most portable electronic devices. [2] Another important

application of LIBs is storage of energy from renewable but intermittent energy sources such as wind and solar. [3] World LIB production reached 500 million units in 2000 and almost 4.6 billion in 2010. [4] Consequently the end-of-life of waste LIB material is becoming an environmental burden. In China, consumer battery waste amounted to 200–500 tons year⁻¹ from 2002 to 2006 with significant amounts of metals, organic chemicals and plastics in the following proportions: 5–20% cobalt, 5–10% nickel, 5–7% lithium, 15% organic chemicals and 7% plastics. This composition varies slightly with different manufacturers [5,6]. Aside from environmental motivations, the price of cobalt (Fig. 1), which fluctuates with the economy but has exhibited a generally increasing trend since 2000, [7] is a strong economic driver to increase LIB recycling. Lithium prices are significantly lower, but have been on the rise since 2006. [8] Therefore, the recycling of spent LIBs has strong potential to provide economic and environmental benefits in

* Corresponding author. Tel.: +86 10 68912508; fax: +86 10 68451429.

** Corresponding author.

E-mail addresses: wufeng863@bit.edu.cn (F. Wu), amine@anl.gov (K. Amine).

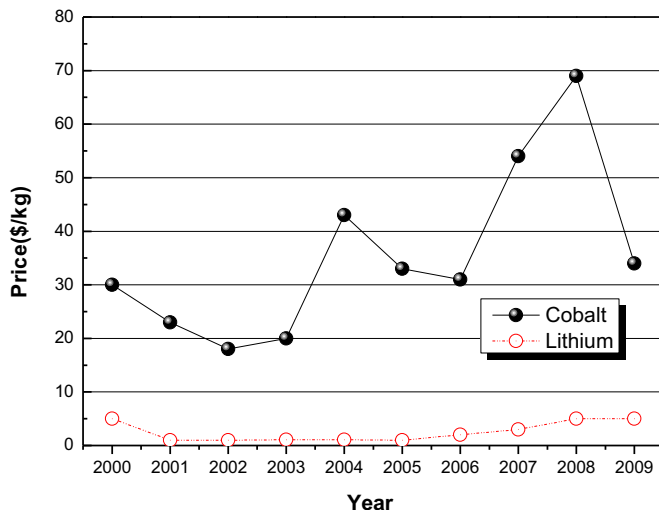


Fig. 1. Prices of lithium and cobalt from 2000 to 2009 [7,8].

addition to conserving raw materials [9–13]. A LIB comprises a cathode, an anode, an organic electrolyte and a separator [14]. The cathode typically consists of Al foil covered by a fine layer of powdered LiCoO_2 , while the anode is made from Cu foil covered by a fine layer of powdered graphitic carbon. Each electrode also contains polyvinylidene fluoride (PVDF), which holds the active material particles together. The electrolyte consists of a Li salt (normally LiPF_6), which is dissolved in an organic solvent. In LIBs, the anodes and cathodes are made from materials that allow the migration of Li ions through an electrolyte solution. The typical chemical composition of LIBs with LiCoO_2 as the cathode active material is shown in Fig. 2 [6].

Recycling processes typically pretreat spent LIBs with physical techniques [10] such as mechanical, thermal, mechanochemical, and dissolution processes. Next, battery components can be recovered via chemical means such as acid leaching or bioleaching, solvent extraction, chemical precipitation and electrochemical processes. Currently, the only large-volume commercial battery recycling technology employs smelting and recovers cobalt and nickel after further processing of smelter output via leaching and solvent extraction [15]. One drawback to this technology is the energy consumption of the high-temperature smelting step and its associated air pollution control equipment. Moreover, it does not recover lithium and aluminum. Acid leaching, on the other hand, is an important technique for recovering valuable metals that avoids these drawbacks. It brings metals into solution, assisted at times by a reductant (e.g., H_2O_2) that converts the metal to a more soluble oxidation state. Once in solution, the metals are more easily separated by electrochemical, precipitation or solvent extraction techniques [6,16,17]. Different leaching agents, such as H_2SO_4 [18], HCl

[19], and HNO_3 [5] have been investigated with lithium and cobalt recoveries exceeding 99%. Notably, strong acid leachants release toxic gases like Cl_2 , SO_3 and NO_x and the waste acid solution is harmful to the environment. To avoid adverse environmental impacts of battery recycling, more benign processes are under development [20].

Similarly, we are developing a low-environmental-impact recycling process using citric ($\text{C}_6\text{H}_8\text{O}_7 \cdot \text{H}_2\text{O}$), DL-malic ($\text{C}_4\text{H}_5\text{O}_6$) and L-aspartic ($\text{C}_4\text{H}_7\text{NO}_4$) acids as leachants to recover metals from spent-battery active materials. The three organic acids were selected because of their characteristics including easy natural degradation and the absence of toxic gases in the reaction process, and because of previous reports of other metal leaching processes [21–24]. The acidity sequence of the three acids is citric acid > malic acid > aspartic acid. They are often used as raw materials in manufacturing. Sonmez and Kumar [21] studied the use of citric acid as a reagent in aqueous media to recover Pb and PbO from scrap battery paste. Wang used malic acid to dissolve the kaolinite in soil [22]. Marafi and Stanislaus [23] conducted ultrasonic-assisted leaching of Mo, V, and Ni from spent hydroprocessing catalysts in citric acid. They determined that citric acid was a superior leachant to H_2SO_4 under the conditions they examined, recovering over 95% of the three metals. Szymczycha-Medea [24] investigated the kinetics of leaching Mo, Ni, V, and Al from spent hydrodesulphurization catalysts in an oxalic acid and hydrogen peroxide solution. We conducted the first preliminary studies into citric acid and DL-malic acid leaching [25,26] of Co and Li from spent-battery active material (LiCoO_2) and have received a patent for this technology [27].

We have now expanded our investigation of acid leaching of spent LIBs to include aspartic acid. The effectiveness of the three organic acids at recovering lithium and cobalt under varying process conditions are compared. Furthermore, we conducted a preliminary study of the acid leaching mechanism. Finally, we conducted an environmental assessment of the process. The two most recent published analyses of LIB [28,29] life-cycle environmental impacts do not include the impacts of battery recycling. While Rydh and Sandén [30] consider the impact of the use of recycled materials on the life-cycle energy consumption of batteries, they do not present an estimate of the energy consumption of the recycling process itself. The data in this paper could be used to address this gap and is a unique examination of the environmental impacts of a battery recycling process.

2. Experimental

2.1. Materials and reagents

Spent LIBs from laptop computers were used in this study. Leachants were citric, DL-malic and L-aspartic acids; hydrogen peroxide (H_2O_2) was the reductant. All solutions were prepared in distilled water and all reagents were analytical grade. To prepare materials for analysis, hydrochloric acid was used to completely leach LiCoO_2 , enabling measurement of the total cobalt and lithium content in the cathode.

2.2. Dismantling, anode/cathode separation and metal characterization

First, cylindrical cells were removed from spent LIBs. Before dismantling the cells, a discharging pretreatment step was used to prevent short-circuiting and self-ignition. The cells were then dismantled using the manual procedure described elsewhere [10] to remove their plastic and steel cases. Once dismantled, the anodes and cathodes were manually uncurled and separated and then the

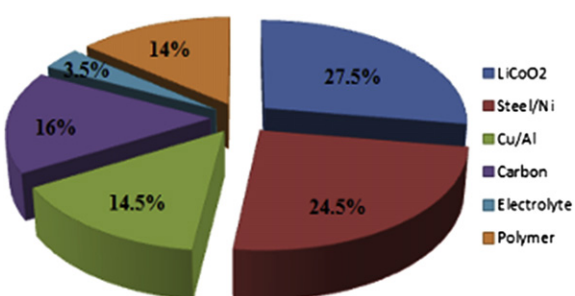


Fig. 2. Chemical composition of a typical lithium-ion secondary rechargeable battery [6].

Table 1

Base case experimental conditions.

Acid	T (°C)	t (min)	[Acid] (M)	[H ₂ O ₂] (vol%)	S:L (g L ⁻¹)
Citric	90	30	1.25	1.0	20
Malic		40	1.5	2.0	20
Aspartic		120	1.5	4.0	10

copper anode foil was recovered. The cathodes were cut into small pieces using scissors and then treated with *N*-methylpyrrolidone (NMP) at 100 °C for 1 h. The cathodic active materials were effectively separated from the aluminum foil and aluminum was recovered in its metallic form. A filtration step recovers the NMP for reuse.

The cathode materials from the spent batteries were calcined at 700 °C for 5 h in a muffle oven to eliminate the carbon and the PVDF in the cathodic active materials, and then cooled to room temperature. Of the steps in this process, the calcination step occurs at the highest temperature and is likely to be the most energy-intensive. The powdered materials were then ground for 2 h in a planetary ball mill to obtain smaller, higher-surface-area particles to increase leaching efficiency. The ground samples were qualitatively and quantitatively analyzed with X-ray diffraction (XRD), scanning electron microscopy (SEM) and inductively coupled plasma atomic emission spectrometry (ICP-AES).

2.3. Metal leaching

The leaching experiments were conducted in a 100-mL three-necked and round-bottomed thermostatic Pyrex reactor placed in a water bath to control the reaction temperature. The reactor was fitted with an impeller stirrer and a vapor condenser to reduce the loss of water by evaporation. A measured amount of waste LiCoO₂ powder and a known strength and quantity of organic acid and H₂O₂ solution were added to the reactor and allowed to reach thermal

equilibrium, with agitation provided by the magnetic stirrer. Reaction conditions were manipulated individually to identify the optimum leaching conditions, i.e., concentrations of organic acid and H₂O₂, solid-to-liquid ratio (S:L), reaction temperature, and reaction time. Base case reaction conditions are provided in Table 1. After the leaching step, the product solution was filtered and washed with distilled water, yielding a pink filtrate and a black residue for analysis. A flow sheet of all the treatment processes is shown in Fig. 3.

2.4. Analytical methods

To determine the total amount of cobalt and lithium in the cathode, an unprocessed sample of the cathodic active material was dissolved completely in concentrated HCl and analyzed by atomic absorption spectrometry (AAS). The amounts of cobalt and lithium in the leaching step filtrate were also measured by AAS to calculate the leaching efficiency, which is defined as the ratio of the amount of a chemical species in the leachate to the total amount of that species in the cathode. Three experiments were conducted simultaneously at all conditions. The values we report are average results from each set of experiments. The cathode materials after calcination and the residues after leaching with different organic acids were characterized using XRD (Rigaku, Cu-K α) and SEM (Hitachi, S-570), respectively. For XRD analysis, the samples were scanned from 10° to 90° using 0.5° steps and a count time of 1 s.

3. Results and discussion

3.1. Dismantling and characterization of the lithium cobalt oxide in spent LIBs

XRD patterns of the spent cathodic materials after calcination and grinding (but before leaching) and the black residues recovered

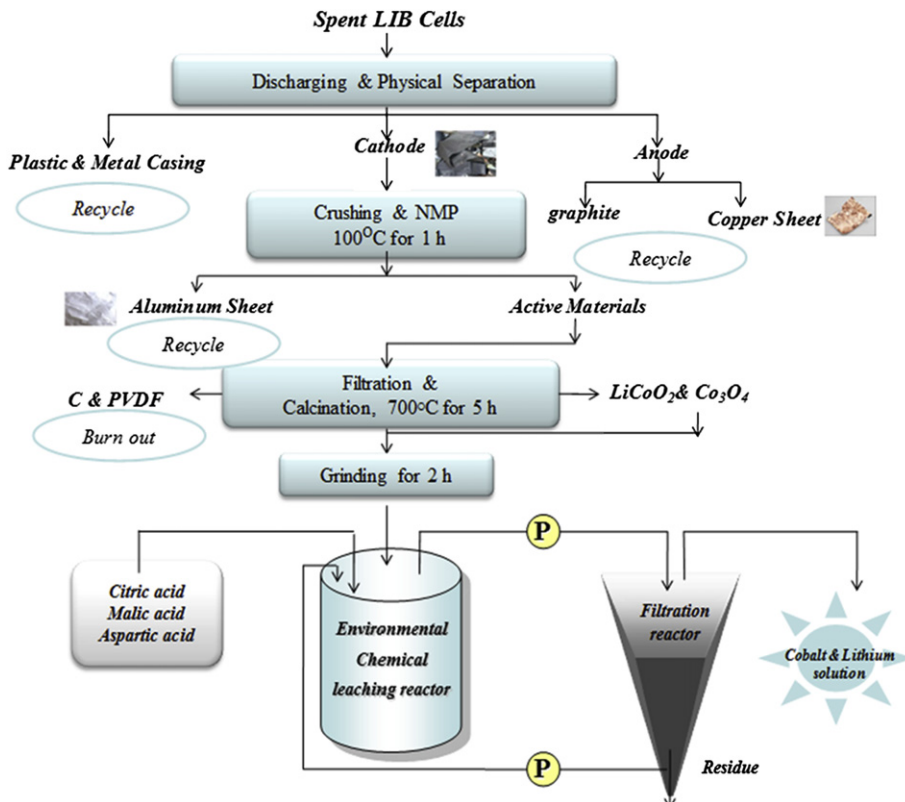


Fig. 3. Flow sheet of the hydrometallurgical recycling process for spent LIBs.

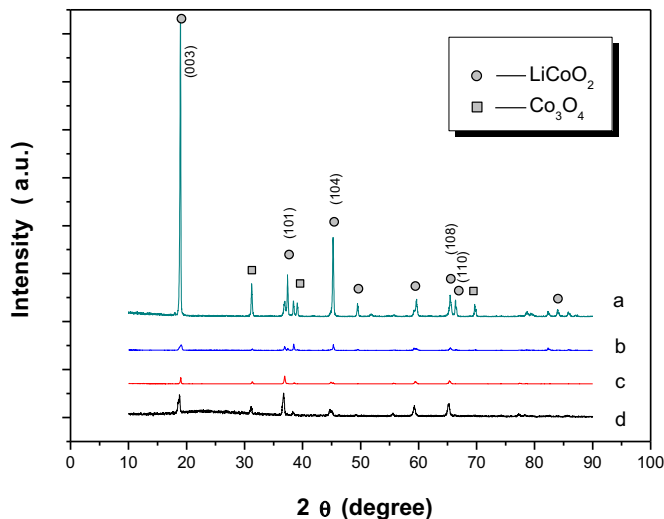


Fig. 4. XRD patterns of samples of (a) the cathodic material after dismantling, calcination and grinding, (b) the residues after citric acid leaching, (c) the residues after DL-malic acid leaching, and (d) the residues after L-aspartic acid leaching. Reaction conditions are reported in Table 1.

from the acid leaching step are shown in Fig. 4. From the XRD data, it is clear that the cathodic materials prior to leaching are mainly LiCoO_2 and small amounts of Co_3O_4 , a performance-reducing degradation product formed during battery operation [31]. The absence of carbon peaks indicates that the calcination process burns off the majority of the carbon residues. As shown by the XRD

data, the bulk of the black residue recovered from citric and malic acid leaching was insoluble Co_3O_4 . On the other hand, low-intensity peaks of LiCoO_2 were identified in the XRD patterns of the residue recovered from leaching with aspartic acid because of incomplete reaction between spent LiCoO_2 and the acid.

Fig. 5 shows SEM images of the spent cathodic materials after calcination and grinding as well as the residues after leaching in the three organic acids. In Fig. 5a, the morphology of the spent cathodic materials was identified as irregular and agglomerated. Leaching reduces the particle size of the unprocessed cathodic materials. By comparison, the particle size of the L-aspartic acid leach residues (Fig. 5d) was larger than that of the other residues (Fig. 5b and c), another indication that the extent of reaction is less when aspartic acid is the leachant.

3.2. Leaching of waste LiCoO_2

As shown in Fig. 6, the leaching reaction of spent LiCoO_2 and the organic acids can be explained in two steps: (1) reduction of $\text{Co}(\text{III})$ to $\text{Co}(\text{II})$ in the presence of H_2O_2 and subsequent dissolution of spent LiCoO_2 in the acid solution; (2) the chelation of $\text{Co}(\text{II})$ and Li with citrate, malate or aspartate. The leaching reaction of the spent LiCoO_2 with citric acid ($\text{C}_6\text{H}_8\text{O}_7$), DL-malic acid ($\text{C}_4\text{H}_6\text{O}_5$) and L-aspartic acid ($\text{C}_4\text{H}_7\text{NO}_4$) is shown in Fig. 7 with some possible products.

3.2.1. Effect of acid concentration on leaching

We studied the effect of acid concentration on the leaching efficiency of waste LiCoO_2 . Although some of the acid will be recoverable, the provision of some amount of makeup acid is likely. The concentration of the three acids was varied from 0.5 to 2 M.

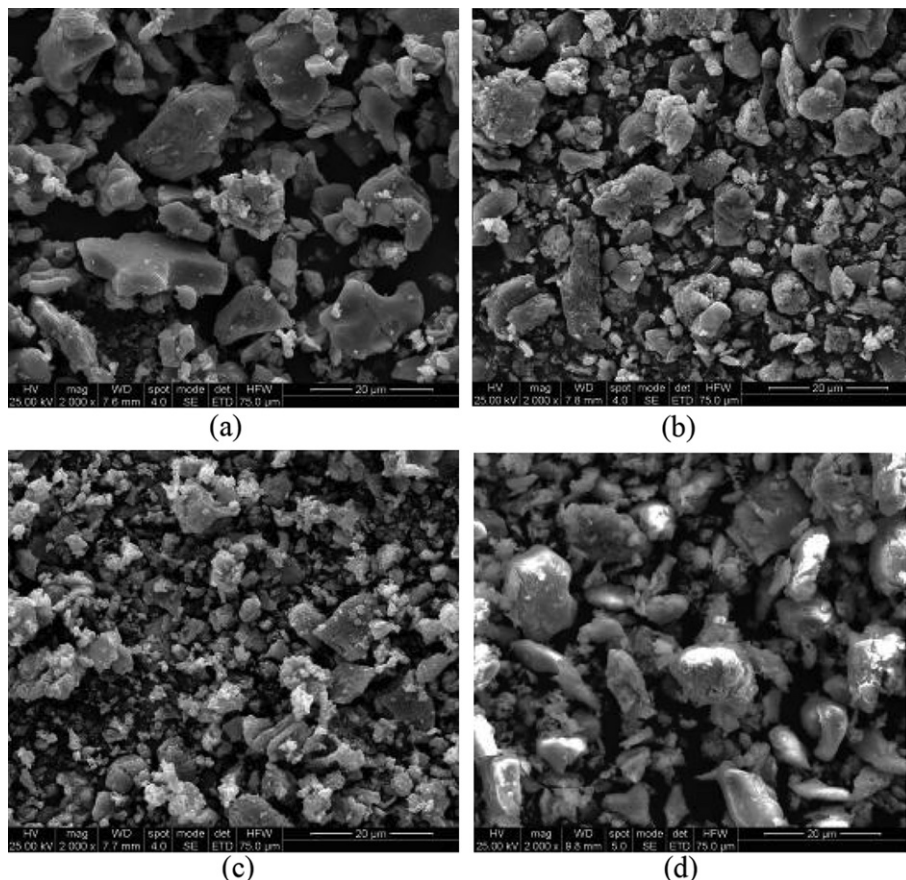


Fig. 5. SEM images of different cathode materials: (a) the cathodic material after dismantling, calcination and grinding, (b) the residues after citric acid leaching, (c) the residues after DL-malic acid leaching, and (d) the residues after L-aspartic acid leaching. Reaction conditions are reported in Table 1.

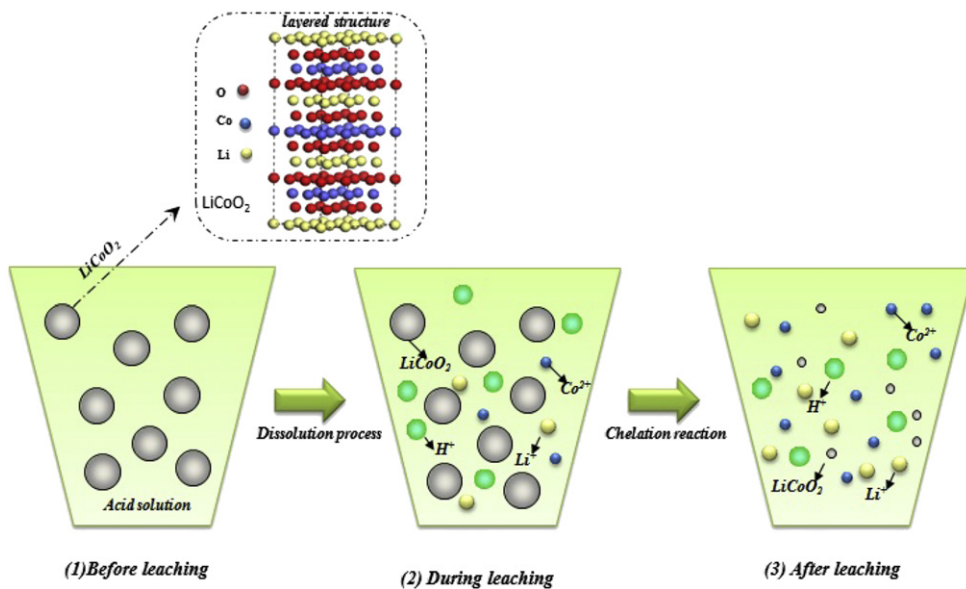


Fig. 6. Possible multiphase leaching reaction of LiCoO_2 particles and organic acid solutions.

Table 1 provides other reaction parameters. We note that in experiments with aspartic acid, small volumes of a dilute NaOH solution were added drop-wise to dissolve the acid in water. Fig. 8 shows that the leaching efficiency of Co and Li initially increased with the acid concentration. More than 90% of Co and nearly 100% of Li were leached as the leachant concentration reached 1.25 M for citric acid and 1.5 M for malic acid. However, approximately 60% of Co and Li were leached when the aspartic acid concentration was increased from 0.5 M to 1.5 M, even though we used a higher reductant concentration in these experiments. When the acid concentration reached 2.0 M, leaching efficiencies of both Co and Li decreased for all acids.

3.2.2. Effect of H_2O_2 on leaching

Products of H_2O_2 decomposition convert Co(III) to Co(II), enhancing the metal's dissolution [32]. The effect of H_2O_2 concentration between 0 and 6 vol.% on leaching is shown in Fig. 9. Other reaction parameters were held at the base case values shown in Table 1. We observed that with citric acid, only 25% of the cobalt and 54% of the lithium were leached in the absence of H_2O_2 , whereas with malic acid 37% of the cobalt and 54% of the lithium were recovered. We also found that with aspartic acid, only about 1% of cobalt and lithium were leached without H_2O_2 and the leaching efficiency of Co and Li increased to 60% as the amount of H_2O_2 was increased to 4.0 vol.%, confirming that H_2O_2 plays an

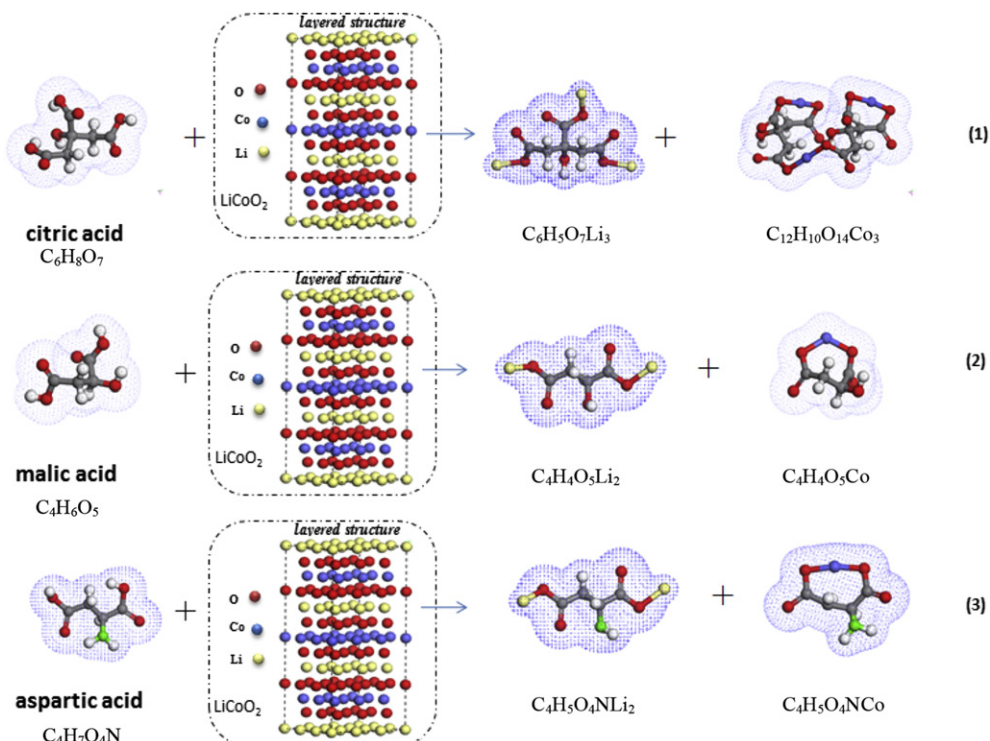


Fig. 7. Possible products of leaching reaction of spent LiCoO_2 with citric acid ($\text{C}_6\text{H}_8\text{O}_7$) (1), DL-malic acid ($\text{C}_4\text{H}_6\text{O}_5$) (2) and L-aspartic acid ($\text{C}_4\text{H}_7\text{NO}_4$) (3).

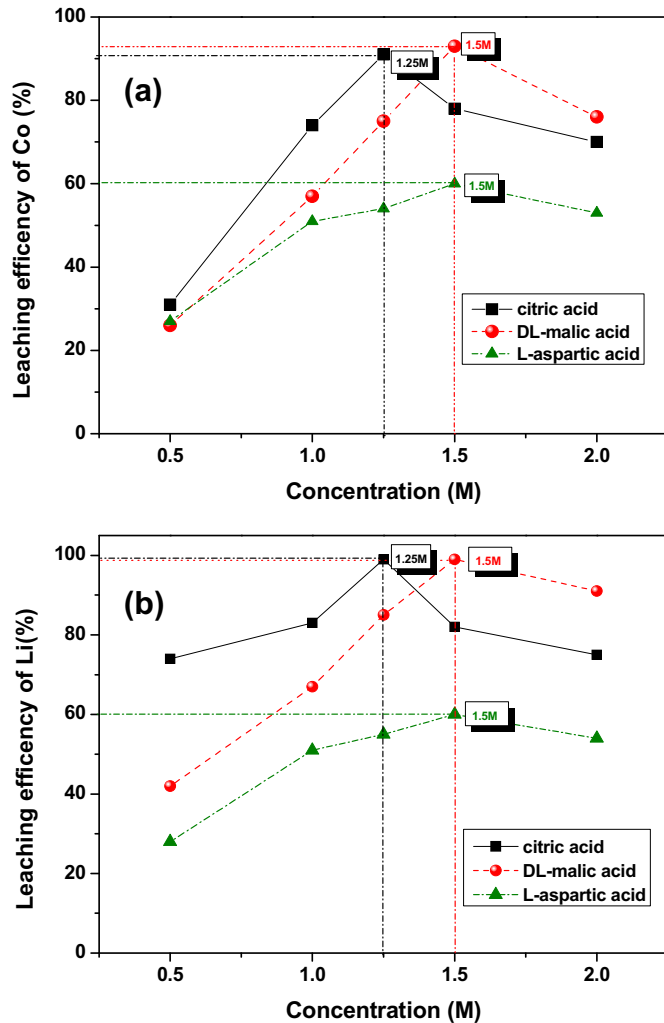


Fig. 8. Effect of acid concentration on the leaching of waste LiCoO_2 : (a) leaching efficiency of Co and (b) leaching efficiency of Li. H_2O_2 concentrations, S:L, and reaction temperature and time are reported in Table 1.

important role in aspartic acid leaching. For citric and malic acids, more than 90% of Co and 99% of Li were leached when the amount of H_2O_2 exceeded 2.0 vol.%. As the amount of H_2O_2 was further increased to 6 vol.%, the increase in leaching efficiency of cobalt and lithium was insignificant.

3.2.3. Effect of the solid-to-liquid ratio on leaching

To examine the effect of S:L on the leaching efficiency, we conducted experiments at S:L from 5 to 30 g L^{-1} . Other reaction parameters were held at the base case values in Table 1. Fig. 10a shows that for citric and malic acids, 91% and 93% of cobalt was leached, respectively, up to an S:L of 20 g L^{-1} . By comparison, at the same S:L, cobalt recovery in aspartic acid was only 36%. Fig. 10b indicates that nearly 100% of lithium was recovered at an S:L of 20 g L^{-1} for citric and malic acids. Exceeding an S:L of 20 g L^{-1} caused these recoveries of cobalt and lithium to decrease dramatically.

3.2.4. Effect of temperature and reaction time on leaching

The energy consumption of the leaching step will be a function of the operating temperature and time. In experiments to examine the effects of these parameters on metal recoveries, the reaction temperature ranged from 25 °C to 90 °C and the reaction time was between 15 and 150 min. Table 1 shows the values of the other

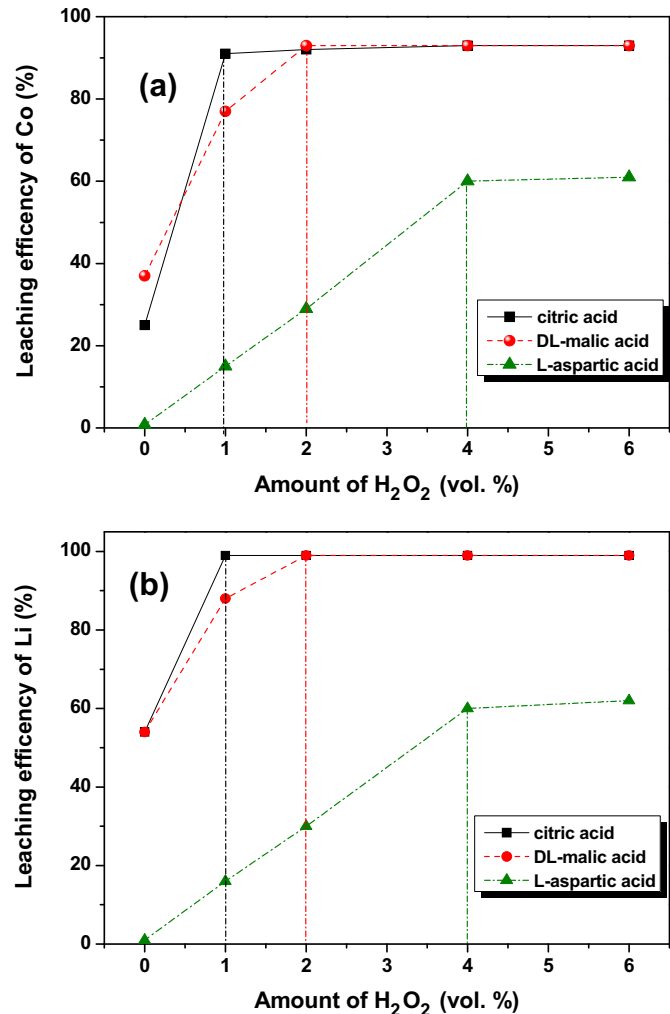


Fig. 9. Effect of H_2O_2 amount on the leaching of waste LiCoO_2 : (a) leaching efficiency of Co and (b) leaching efficiency of Li. Acid concentrations, S:L, and reaction temperature and time are reported in Table 1.

reaction parameters. The effect of reaction temperature and time on leaching is shown in Fig. 11. At 20 °C, cobalt recoveries were only 8%, 17% and 12% for citric, malic and aspartic acid leaching, respectively (Fig. 11a). Leaching efficiency improved with increasing temperature. At 90 °C, leaching in citric, malic and aspartic acids achieved cobalt recoveries of 92%, 93% and 60%, respectively. Lithium leaching followed the same trend, as Fig. 11b illustrates. Collectively, these results show that up to about 90 °C, higher reaction temperatures enhance metal leaching. One explanation for this trend is the endothermicity of leachant dissociation, which translates to greater acid dissociation and increased reaction rates at elevated temperatures. Above 90 °C, however, the acids begin to volatilize. With less leachant in solution, metal recoveries decrease.

Additionally, we observed that in citric acid, metal recovery was highest (99%) after 30 min under the base case conditions shown in Table 1. The optimal reaction time in malic acid was 40 min under the base case conditions. In aspartic acid, recovery reached only 27% after 30 min under base case conditions. A longer reaction time (2 h) did increase recovery of cobalt and lithium, but only to 60%. Reactions in aspartic acid likely achieve lower recovery rates than in the other acids in this study because it is the least acidic.

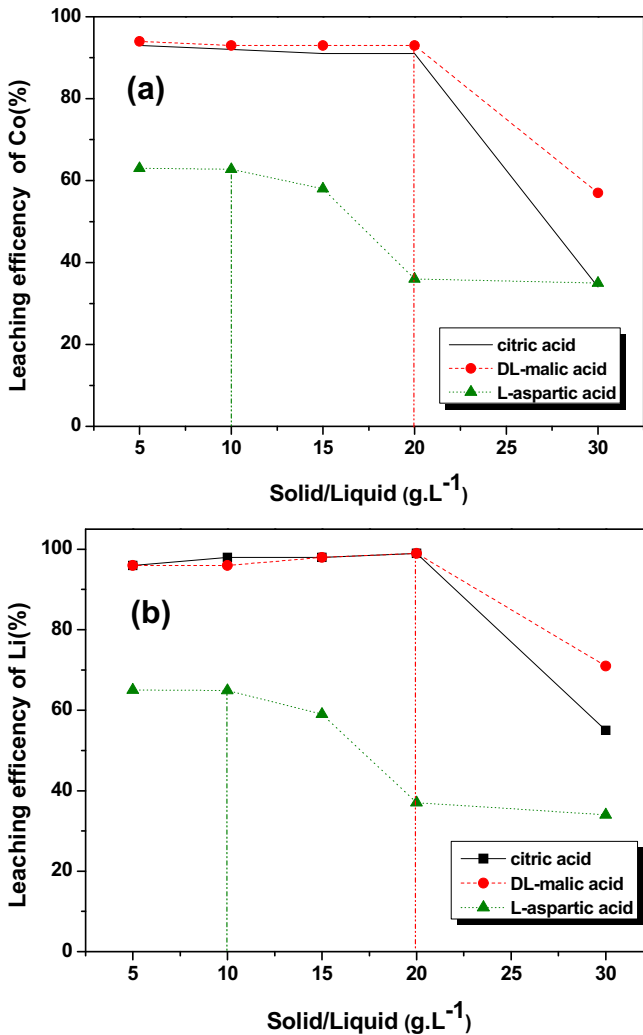


Fig. 10. Effect of the solid/liquid ratio on the leaching of waste LiCoO_2 : (a) leaching efficiency of Co and (b) leaching efficiency of Li. Acid and H_2O_2 concentrations, reaction temperature, and reaction time are reported in Table 1.

4. ENVIRONMENTAL ASSESSMENT

In addition to economic and, in Europe, regulatory motivations, one key driver for recycling batteries is to reduce their environmental burden. In this section, we describe our environmental analysis of this recycling process. Our results have four potential uses. First, they can identify the highest-energy-consuming steps of this process and inform efforts to reduce process energy intensity. Second, they can be used in comparing the energy intensities of battery recycling process alternatives. Third, they can be compared to the energy intensity of producing active materials from virgin compounds (e.g., lithium salts from Chile). If, in recovering a battery component, the recycling process consumes more energy than producing that component from virgin materials, it likely does not reduce battery life-cycle energy consumption. Recycling the component would, however, conserve possibly limited raw materials. Finally, these results can be incorporated into a life-cycle analysis of an LIB.

The boundary of this analysis is in Fig. 12. One key factor in this analysis is the choice of leachant. We note that consumption of the reductant and leachant will impact the life-cycle energy use of leaching process because their production incurs environmental burdens. The life-cycle pathways for the three organic acids in the

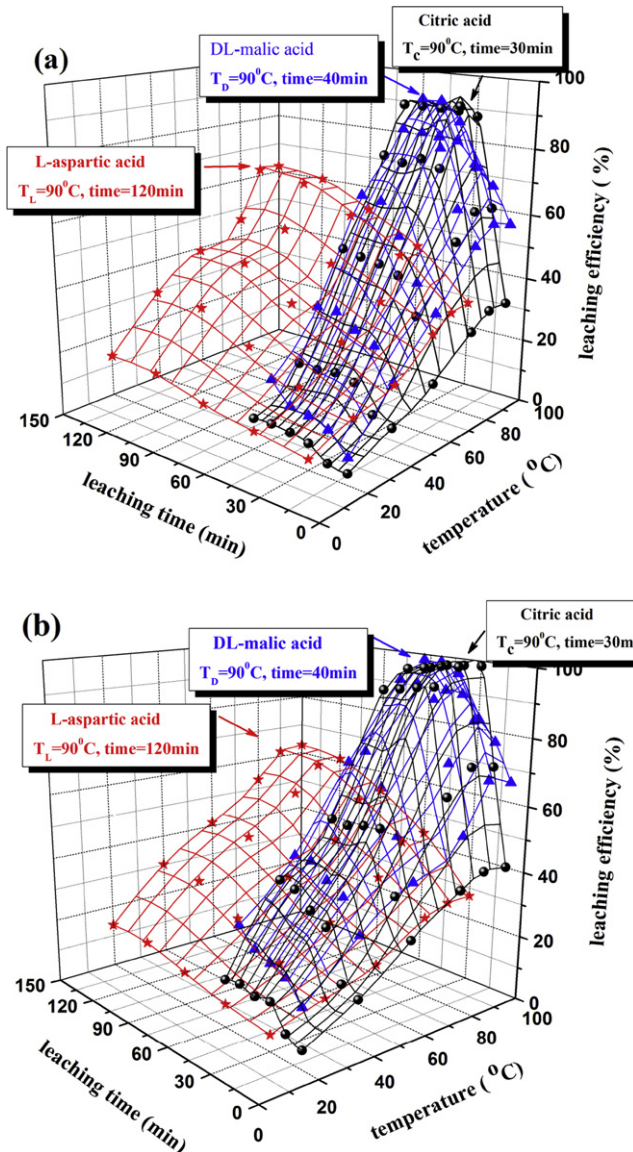


Fig. 11. Effect of temperature and time on the leaching of waste LiCoO_2 : (a) leaching efficiency of Co and (b) leaching efficiency of Li. Acid and H_2O_2 concentrations and S:L are reported in Table 1.

experimental work are shown in Fig. 13. Malic and aspartic acids come from the same production chain, which begins with fossil-derived butane. On the other hand, citric acid comes from the fermentation of cornstarch produced from corn wet-milling. Comparing the energies associated with the feedstocks of these acids provides insight into which acid will have the least impact on the overall energy consumption of the recycling process (as defined in Fig. 12). On a fossil energy content basis, the energy consumed to produce butane (including its inherent energy) is approximately 10 times that of corn, the raw material for citric acid [34]. Further, citric acid production entails fewer steps than the production of malic and aspartic acids. We therefore selected citric acid as the leachant in our analysis and adopted an energy consumption of 35 MJ kg⁻¹ for the entire pathway of citric acid production, as developed in the Supporting information.

In our calculations of process energy intensity, we used the optimal reaction temperature, reaction time, and peroxide concentrations for the recycling process as determined in the experimental work. We based acid concentration on stoichiometry

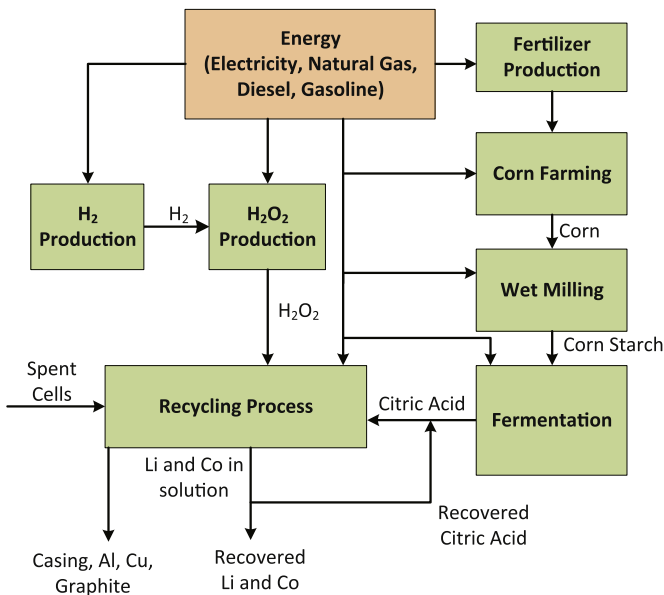


Fig. 12. Recycling process environmental analysis boundary.

as described in the *Supporting Information*. We used energy consumption values calculated from analysis of existing industrial processes rather than use the energy consumption of the laboratory equipment. This approach is preferable because the laboratory-scale process is not optimized, as an industrial process would be, to minimize energy consumption while optimizing throughput. In the *Supporting information*, we detail the calculation methods and data sources we used to generate the results we present here.

Fig. 14 displays the purchased energy intensity of each step of the recycling process per mass of recovered cobalt. (Purchased energy intensity is the energy content of the fuel used on-site at the recycling plant.) The shares of natural gas and electricity for the overall process are 49% and 51%, respectively. We chose to report results on the basis of mass of recovered cobalt rather than lithium because cobalt is the more valuable metal. Logically, the high-temperature calcination step is the most energy-intensive in this process. It also emits carbon dioxide (from combustion of the PVDF and graphite) at a level of $2660 \text{ g CO}_2 \text{ kg}^{-1}$ recovered Co. Production of virgin CoO emits over five times this amount of GHGs [34]. The calcining step will also release the fluorine in PVDF, likely as HF, and we do not account for these emissions or their control. Scrubbers can reduce HF emissions by 99% [35]. After calcining, crushing and grinding were the next most significant energy consumers. Increasing the cobalt recovery efficiency from 60% to 90% through use of the more effective leachants decreases purchased energy consumption by 35%.

We incorporated the purchased energy data for the recycling process and the production of H_2O_2 and citric acid (see *Supporting*

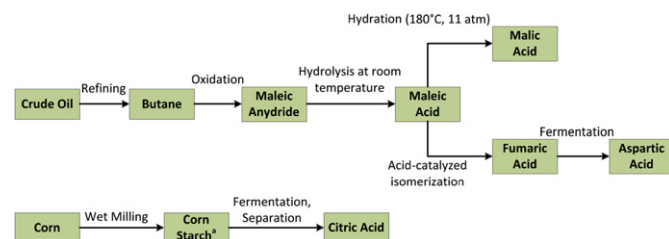
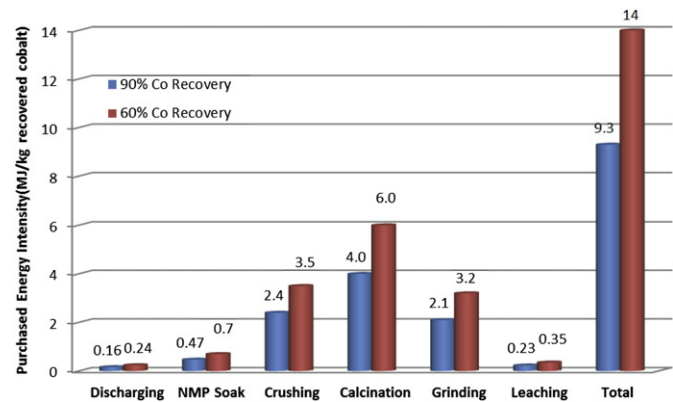


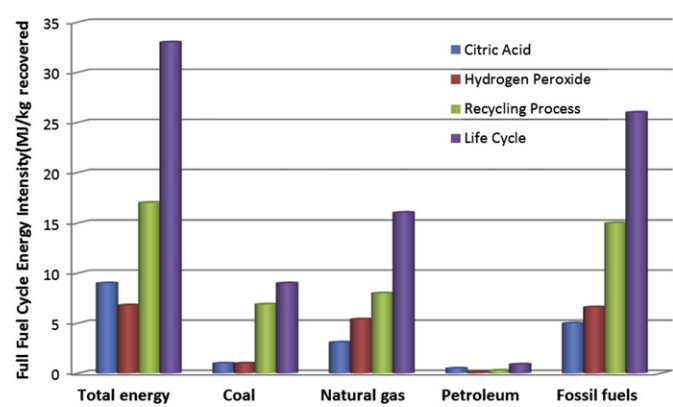
Fig. 13. Production pathways for citric, malic, and aspartic acids. ^aCorn starch is the major feedstock for citric acid production in the U.S. [33]. In China, sweet potato and cassava are primary feedstocks.

Fig. 14. Purchased energy intensity (MJ kg^{-1} recovered Co) of the recycling process.

information) into Argonne National Laboratory's Greenhouse Gases, Regulated Emissions, and Energy use in Transportation (GREET) model [34], which calculates the full fuel cycle (FFC) energy consumption from these data. (FFC energy consumption accounts for upstream steps, such as coal mining, that consume energy in the production chain that precedes the delivery of purchased energy.) Fig. 15 displays the FFC energy intensity of the recycling process and the product feeds (citric acid and hydrogen peroxide) in units of MJ kg^{-1} recovered Co at 90% Co recovery.

Fig. 15 illustrates the significant impact of citric acid on the total energy consumption of the recycling process. In our analysis, we assume that it is possible to recover 90% of the acid for recycling by decreasing the solution pH, causing the metals to precipitate [36]. After filtration, acid recovery can certainly be feasible, possibly at rates above 90%. Although it is desirable to limit waste quantities, waste citric acid would not pose a serious environmental threat because it is a relatively benign substance that is used in foods, beverages, and detergents.

The total energy consumption for the recycling process (including the impacts of organic acid and H_2O_2 consumption) is 33 MJ kg^{-1} . As the process is further developed, opportunities exist to increase process energy efficiency, for example, by lowering the calcining temperature, further optimizing acid and peroxide concentrations, and maximizing acid recycling. Fig. 16 contains the FFC GHG emissions for provision of the organic acid and hydrogen peroxide in addition to emissions from the recycling process itself. The latter includes process CO_2 emissions from the calcining step (55% of FFC GHG CO_2e emissions). We also calculated corresponding emissions of other air pollutants (volatile organic compounds,

Fig. 15. FFC energy intensity for organic acid, hydrogen peroxide and the recycling process for 90% recovery of Co (MJ kg^{-1} recovered Co).

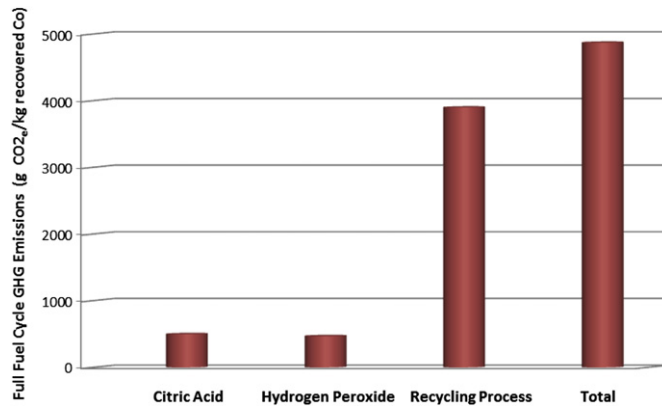


Fig. 16. FFC GHG emissions from organic acid and hydrogen peroxide production and the recycling process (g CO₂e kg⁻¹ recovered Co) for 90% cobalt recovery.

carbon monoxide, nitrous oxides, particulate matter, sulfur oxides, methane, and nitrous oxide) and report them in the *Supporting information*.

We note that the recovered Li and Co would need to undergo further processing to yield an active material for integration into an LIB. We have not yet estimated the energy intensity of this additional processing. However, Majeau-Bettez et al. [29] report the energy intensity of nickel–cobalt–manganese–oxide cathode material manufacturing (including acquisition and processing of virgin materials) as 132 MJ kg⁻¹. These authors do not isolate the contribution of Co acquisition and processing, so a direct assessment of whether obtaining cobalt from spent LIB leaching or from virgin materials is less energy-intensive is not feasible. The process we have analyzed, however, has a FFC energy intensity roughly 25% of the value that Majeau-Bettez et al. [29] report. Similarly, producing virgin cobalt oxide could be up to six times more energy-intensive than obtaining Co from this recycling process [34]. It seems possible, then, that the recycled cobalt could be integrated into the cathodic material without increasing, and conceivably decreasing the energy intensity of its production.

We are unable to fully compare the energy intensity of this battery recycling process to that of another because published data on the energy intensity of these processes is limited. From a preliminary analysis on a per mass of cobalt recovered basis, however, the FFC energy intensity of this process may exceed that of the production of cobalt salts through a smelting-based commercial battery recycling process described elsewhere [15]. The hydrometallurgical process, however, can recover both lithium and cobalt whereas lithium is unrecoverable in the smelting-based process. Additionally, as process parameters for the hydrometallurgical process become more optimized its energy intensity is likely to decrease.

Although we present results in this section without associated uncertainties, there are a number of variables that significantly affect the results. First, because the recycling process is under development in the laboratory, data for its energy consumption do not exist on an industrial scale. We estimated this intensity, which will undoubtedly change with technology implementation. Second, material intensity will also likely change upon adoption of this process on an industrial scale. Moreover, as we describe in the *Supporting information*, the data used for citric acid production is largely based on the wet-milling process for corn ethanol. Production of citric acid may be more or less energy-intensive. Clearly, it is crucial to recycle as much of the acid as possible both to minimize waste and to reduce the FFC energy intensity of the process. Finally, using citric acid enables this process to be competitive with producing virgin cobalt on an energy consumption

basis. If a fossil-derived organic acid were used, the environmental benefits of this process would require re-evaluation.

5. Conclusions

Spent LIBs can be deleterious to the environment and, importantly, could be a source of materials (Li, Co, aluminum, copper) for new batteries. Battery recycling therefore promises significant environmental and economic benefits. In this paper, we expanded our ongoing exploration of acid leaching of Co and Li from LIBs to include L-aspartic acid. On a molecular level, organic acid leaching mechanisms likely include dissolution and chelation.

In this investigation, recoveries of nearly 100% of Li and in excess of 90% of Co were achieved following leaching in citric or malic acids. Aspartic acid was significantly less effective because of its weak acidity and lower solubility in water. We found that the leaching efficiency of both Co and Li were high at a temperature of 90 °C. High recoveries from leaching in citric and malic acids were achieved at much shorter reaction times (30–40 min) than in aspartic acid (2 h). An S:L of 20 g L⁻¹ resulted in the best cobalt and lithium recoveries from leaching in citric and malic acids; increasing the ratio beyond 20 g L⁻¹ caused metal recoveries to decrease. The H₂O₂ concentration also significantly influenced metal recovery. Finally, an environmental analysis of this process predicts a FFC energy intensity of 33 MJ kg⁻¹ of recovered Co when the Co recovery efficiency is 90% and the leachant is citric acid.

Acknowledgments

The experimental work of this study was supported by the International S&T Cooperation Program of China (2010DFB63370), the Chinese National 973 Program (2009CB220106), Beijing Nova Program (Z121103002512029), Beijing Excellent Youth Scholars funding, and the New Century Educational Talents Plan of the Chinese Education Ministry (NCET-12-0050). The analysis work, especially the life-cycle analysis work, was supported by the Vehicle Technology Program of the Office of Energy Efficiency and Renewable Energy, U.S. Department of Energy, under contract DE-AC02-06CH11357. The authors would like to thank Dr. Michael Wang and Dr. John Sullivan of Argonne National Laboratory for helpful discussions in the development of this paper.

Appendix A. Supplementary data

Supplementary data related to this article can be found at <http://dx.doi.org/10.1016/j.jpowsour.2012.12.089>.

References

- [1] R. Moshtev, B. Johnson, J. Power Sources 91 (2000) 86–91.
- [2] V. Etacheri, R. Marom, R. Elazari, G. Salitra, D. Aurbach, Energy Environ. Sci. 4 (2011) 3243–3262.
- [3] B. Scrosati, J. Hassoun, Y.-K. Sun, Energy Environ. Sci. 4 (2011) 3287–3295.
- [4] UMICORE, Materials Technology Group. Available at: <http://www.uminicore.com> (accessed 28.08.12).
- [5] C.K. Lee, K.I. Rhee, Hydrometallurgy 268 (2003) 5–10.
- [6] S.M. Shin, N.H. Kim, J.S. Sohn, D.H. Yang, Y.H. Kim, Hydrometallurgy 79 (2005) 172–181.
- [7] USGS, Cobalt Statistics. Available at: <http://minerals.usgs.gov/ds/2005/140/cobalt.pdf> (accessed 28.08.12).
- [8] USGS, Lithium Statistics. Available at: <http://minerals.usgs.gov/ds/2005/140/lithium.pdf> (accessed 28.08.12).
- [9] S. Catillo, F. Ansart, C. Laberty-Robert, J. Portal, J. Power Sources 112 (2002) 247–254.
- [10] J. Xu, H.R. Thomas, R.W. Francis, K.R. Lum, J. Wang, B. Liang, J. Power Sources 177 (2008) 512–527.
- [11] E.M. García, J.S. Santos, E.C. Pereira, M.B.J.G. Freitas, J. Power Sources 185 (2008) 549–553.
- [12] J.F. Paulino, N.G. Busnardo, J.C. Afonso, J. Hazard. Mater. 150 (2008) 843–849.
- [13] T. Kanamori, M. Matsuda, M. Miyake, J. Hazard. Mater. 169 (2009) 240–245.

- [14] P.A. Nelson, K.G. Gallagher, I. Bloom, D.W. Dees, Modeling the Performance and Cost of Lithium-ion Batteries for Electric-drive Vehicles, Argonne National Laboratory, 2011, Report ANL-11/32.
- [15] L. Gaines, J. Sullivan, A. Burnham, I. Belharouak, Life-cycle Analysis for Lithium-ion Battery Production and Recycling, in: 90th Annual Meeting, January 2011, Transportation Research Board, 2011, paper 11-3891.
- [16] C. Lupi, M. Pasquali, A. Dell'Era, Waste Manag. 25 (2005) 215–220.
- [17] B. Swain, J. Jeong, J.C. Lee, G.H. Lee, J.S. Sohn, J. Power Sources 167 (2007) 536–544.
- [18] P.M. Danuza, D. Germano, C.A.E. Renata, B.M. Marcelo, J. Power Sources 159 (2006) 1510–1518.
- [19] P. Zhang, T. Yokoyama, O. Itabashi, T.M. Suzuki, K. Inoue, Hydrometallurgy 47 (1998) 259–271.
- [20] S. Saeki, J. Lee, Q.W. Zhang, F. Saito, Int. J. Miner. Process. 74S (2004) S373–S378.
- [21] M.S. Sonmez, R.V. Kumar, Hydrometallurgy 95 (2009) 53–60.
- [22] X.X. Wang, Q.M. Li, H.F. Hu, J. Colloid Interface Sci. 290 (2005) 481–488.
- [23] M. Marafi, A. Stanislaus, Ind. Eng. Chem. Res. 50 (2011) 9495–9501.
- [24] A. Szymczycha-Madeja, J. Hazard. Mater. 186 (2011) 2157–2161.
- [25] L. Li, J. Ge, F. Wu, J. Hazard. Mater. 176 (2010) 288–293.
- [26] L. Li, J. Ge, R. Chen, Waste Manag. 30 (2010) 2615–2621.
- [27] China Patent, ZL 200910093727.8, 2011.
- [28] D.A. Notter, M. Gauch, R. Widmer, P. Wäger, A. Stamp, R. Zah, H.J. Althaus, Environ. Sci. Technol. 44 (2010) 6550–6556.
- [29] G. Majeau-Bettez, T.R. Hawkins, A.H. Strømman, Environ. Sci. Technol. 45 (2011) 4548–4554.
- [30] C.J. Rydh, B.A. Sandén, Energy Convers. Manag. 46 (2005) 1957–1979.
- [31] M.B.J.G. Freitas, E.M. Garcia, J. Power Sources 171 (2007) 953–959.
- [32] G. Dorella, M.B. Mansur, J. Power Sources 170 (2007) 210–215.
- [33] M.P. Malveda, H. Janshekar, Y. Inoguchi, Citric Acid, Chemical Economics Handbook Marketing Research Report, 2009.
- [34] Argonne National Laboratory GREET Model, <http://greet.es.anl.gov/>.
- [35] U.S. Environmental Protection Agency, AP-42, Hydrofluoric Acid, <http://www.epa.gov/ttnchie1/ap42/ch08/08/final/c08s07.pdf>, 1995 (accessed 28.08.12) (Chapter 8.7).
- [36] Kirk-Othmer Encyclopedia of Chemical Technology, <http://dx.doi.org/10.1002/0471238961>.